

Te doping of GaInP: Ordering and step structure

S. H. Lee, C. Y. Fetzer, and G. B. Stringfellow^{a)}

Department of Materials Science and Engineering, University of Utah, Salt Lake City, Utah 94112

D. H. Lee and T. Y. Seong

Department of Materials Science and Engineering, Kwangju Institute of Science and Technology, Kwangju 506-712, Korea

(Received 28 September 1998; accepted for publication 23 December 1998)

The donor Te has been added to GaInP during organometallic vapor phase epitaxial growth using the precursor diethyltelluride. In agreement with previous studies, the addition of high Te concentrations leads to the elimination of the CuPt ordering observed in undoped layers. The degree of order is estimated from the low temperature photoluminescence peak energy to decrease from 0.5 at Te concentrations of $<2 \times 10^{17} \text{ cm}^{-3}$ to 0 for Te concentrations of $>6 \times 10^{17} \text{ cm}^{-3}$. This is verified by transmission electron diffraction studies, which show the elimination of the $1/2\{111\}$ superlattice spots at high Te doping levels. A remarkable change in the surface structure is found to accompany this decrease in ordering: The surfaces become much smoother. Step bunching is observed to disappear for the vicinal GaAs substrates, misoriented from (001) by 3° in the B direction, and three-dimensional island (or mound) formation is eliminated for the singular (001) substrates. A qualitative model is presented explaining this behavior based on the effect of Te on the step structure and the bonding at step edges, both of which affect the adatom sticking at steps.

© 1999 American Institute of Physics. [S0021-8979(99)01807-1]

I. INTRODUCTION

A remarkable phenomenon occurs during the vapor phase epitaxial growth of semiconductor alloys on (001) oriented substrates. The CuPt ordered structure, consisting of alternating $\{111\}B$ monolayers of the two binary components, occurs for virtually all III/V semiconductor alloys, as well as for II–VI and Ge–Si alloys.¹ In particular, formation of the CuPt structure frequently occurs in $\text{Ga}_{0.515}\text{In}_{0.485}\text{P}$ layers grown by organometallic vapor phase epitaxy (OMVPE).² This ordered structure is not stable in the bulk alloy. Theoretically, the alternating surface stresses resulting from the formation of $[\bar{1}10]$ -oriented phosphorous dimers on the $(2 \times n)$ reconstructed (001) surface, often formed during OMVPE growth of InP and GaInP,³ thermodynamically stabilize the variants of the CuPt structure with ordering on the $(\bar{1}11)$ and $(1\bar{1}1)$ planes in the region just below the surface.^{2,4} This is verified experimentally by the observed 1:1 correlation between the P dimer concentration and the degree of order with increasing temperature and decreasing partial pressure of the P precursor.⁵

This phenomenon is of considerable practical interest since ordering has a large effect on the materials properties. For example, the band gap energy is found to be 160 meV lower in partially ordered $\text{Ga}_{0.515}\text{In}_{0.485}\text{P}$ than in disordered material of the same composition.⁶ This is very important for visible light emitting diodes and injection laser diodes. Ordering must be avoided in order to produce the shortest wavelength devices. On the other hand, ordering offers the attractive possibility of producing heterostructures⁶ and

quantum wells⁷ by changing the band gap energy without altering the solid composition.

A study of the effect of substrate misorientation on the kinetics of ordering suggests that the step structure is also important: $[110]$ steps assist ordering and $[\bar{1}10]$ steps retard ordering.⁸ However, the mechanistic role of steps remains unclear.

In addition to the effects of the growth parameters, doping is also found to have a pronounced effect on the degree of order produced in GaInP during OMVPE growth. Both n - and p -type doping have been demonstrated to reduce CuPt ordering.^{9–15} The mechanism for this effect also remains unknown. Previous work in our group has shown that the addition of Te during OMVPE growth affects both step structure and ordering.^{16,17}

The purpose of this article is to further describe the effect of the addition of the donor Te during the OMVPE growth of GaInP on the degree of CuPt order and on the step structure, determined using atomic force microscopy (AFM) techniques and to advance a model for the phenomena observed. This is a part of a broader effort aimed at obtaining a better understanding of the ordering process occurring at the surface during epitaxial growth, particularly the role of steps.

II. EXPERIMENTAL PROCEDURE

Te-doped GaInP layers were grown by OMVPE in a horizontal, infrared-heated, atmospheric pressure reactor using trimethylindium (TMIn), trimethylgallium (TMGa), and tertiarybutylphosphine (TBP) with diethyltelluride (DETe) as the dopant precursor on semi-insulating GaAs substrates with both singular (001) and vicinal 3_B° (3° toward $(111)B$ direction) orientations. The DETe was diluted to 5 ppm in

^{a)}Electronic mail: stringfellow@ee.utah.edu

H₂. The carrier gas was Pd-diffused hydrogen. The total flow was a constant 4360 sccm. Substrate preparation consisted of degreasing followed by a 1 min etch in a 2:12:1 solution of NH₄OH, H₂O, and H₂O₂. Before beginning the GaInP growth, a 0.05 μm GaAs buffer layer was deposited to improve the quality of the GaInP layer. The GaInP thickness was about 0.3 μm for all samples. The growth rate was 0.6 μm/h and the growth temperature was 670 °C. The TBP partial pressure and V/III ratio were kept constant at 3.0 Torr and 180, respectively. After completing the growth, the group III precursors were removed and the samples were cooled, with an initial cooling rate of approximately 70 °C/min.

The free electron concentration and mobility were measured at room temperature using the Hall effect with the van der Pauw geometry. Ohmic contacts were formed using indium dots alloyed for 10 min at 300 °C in N₂. The solid composition of the GaInP layers was determined using Vegard's law, from x-ray diffraction measurement using Cu Kα radiation. Only results for lattice matched layers, with values of GaP concentration in the solid of 0.515, are presented here. The 20 K photoluminescence (PL) was excited with the 488 nm line of an Ar⁺ laser. The emission was dispersed using a Spex Model 1870 monochromator and detected using a Hamamatsu R1104 head-on photomultiplier tube.

For electron microscope examination, [110] cross-sectional transmission electron microscope (TEM) samples were prepared using standard Ar⁺ ion milling at 77 K. The transmission electron diffraction (TED) patterns were obtained using a JEM 2010 instrument operated at 200 KV. The thicknesses of the thin foils examined by TEM were in the range 150–400 nm.

The surface structure was characterized using a Nanoscope III AFM in the tapping mode. Etched single-crystalline Si tips were used with an end radius of about 5 nm, with a sidewall angle of about 35°. Scan rates of 1–2 lines per second were used and data were taken at 512 points/line and 512 lines per scan area. The samples were measured in air, so were covered by a thin, conformal oxide layer.

III. RESULTS

The 20 K PL peak energy was used to estimate the band gap energy for the GaInP layers, all lattice matched to the GaAs substrate. The resultant energies for layers grown on singular (001) and vicinal (3_B⁰) substrates are plotted versus the free electron concentration due to Te doping in Fig. 1. The band gap energy of disordered GaInP lattice matched to GaAs is known to be approximately 2.0 eV.¹⁸ As seen in Fig. 1, this is the PL peak energy observed for the layers doped with Te to concentrations of >8 × 10¹⁷ cm⁻³. For undoped layers and those with Te concentrations of ≲2 × 10¹⁷ cm⁻³ the band gap energy is 110 meV lower, at approximately 1.89 eV. Two factors might contribute to the blue shift in the PL peak energy with increasing Te doping level. Filling of the conduction band is known to shift the PL peak energy to higher energies.¹⁹ In addition, a decrease in the order parameter will also cause a large blue shift.¹⁸ To estimate the magnitude of the band filling effect, the PL peak energy was

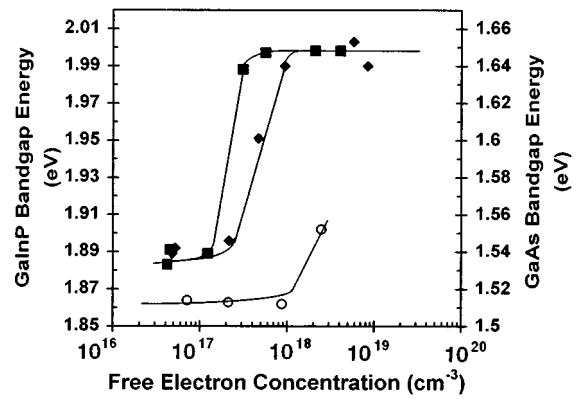


FIG. 1. PL peak energy vs electron concentration from Te doping. GaInP (001) singular layers (◆) and vicinal layers (■) were grown at 670 °C. Data points (○) for Te-doped GaAs (001) vicinal layers (3_B⁰ misorientation) grown at 620 °C are shown for comparison. The lines were simply drawn to fit the data points.

measured for GaAs layers versus the free electron concentration due to Te doping. The results, also plotted in Fig. 1, indicate that over the range of Te doping causing the 110 meV shift in the PL peak energy, the GaAs peak position is nearly constant. Since the conduction band density of states is larger in GaInP than in GaAs, due to the larger effective mass,²⁰ band filling will begin at higher electron concentrations in GaInP. This suggests that the most important effect is due to loss of the CuPt ordered structure due to Te doping.

A more direct, but nonquantitative, measure of the degree of order is obtained from TED patterns. Figure 2(a) shows the TED pattern for the GaInP layers doped to 4.2 × 10¹⁶ cm⁻³ grown on the vicinal substrate orientation. In addition to the normal zincblende lattice spots, sharp spots are obtained at the 1/2(1̄11) position. The spots are very intense, consistent with the high degree of order, approximately 0.5, deduced from the PL peak energy. Only a single variant is formed due to the presence of [110] steps caused by the substrate misorientation.²¹ The CuPt superspot intensities are significantly decreased in Fig. 2(b) for a Te doping level of 3.1 × 10¹⁷ cm⁻³. The superlattice spots have disappeared for a free electron concentration due to Te doping of 2.1 × 10¹⁸ cm⁻³. A similar decrease in the superspot intensities with increasing Te doping occurs for the singular (001) samples, as seen in Figs. 2(d)–2(f). Figure 2(d) indicates the presence of the two B variants of the CuPt structure, as is common for singular (001) substrates.

The degree of order, S, deduced from the calculated dependence of the 20 K PL peak energy on the degree of CuPt order in GaInP lattice matched to GaAs¹⁸

$$S = \{ [2005 - \text{PL peak energy at 20 K (in meV)}] / 471 \}^{1/2}, \quad (1)$$

is plotted versus the free electron concentration due to Te doping in Fig. 3(a). For both singular and vicinal substrates, the degree of order drops significantly as the Te concentration increases from 10¹⁷ to 10¹⁸ cm⁻³. The Te concentrations necessary to destroy the CuPt order are seen to be slightly (approximately a factor of 2) higher for the singular (001) oriented samples than for the vicinal samples.

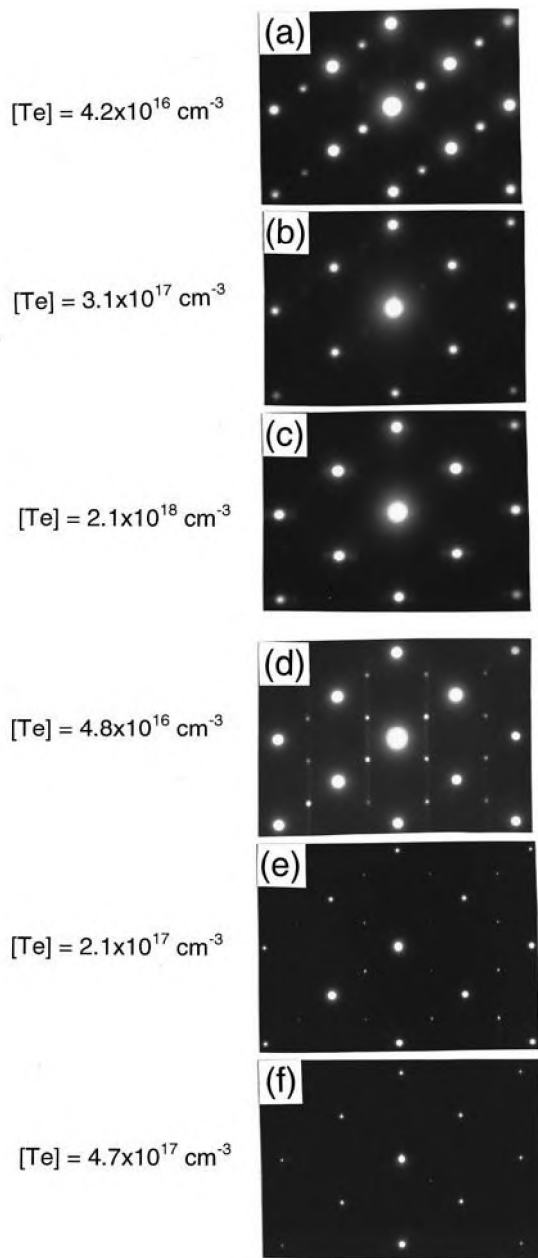


FIG. 2. [110] TED patterns taken from Te-doped GaInP layers grown at 670 °C with various doping concentrations. Figs. 2(a)–2(c) are vicinal layers and Figs. 2(d)–2(f) are singular (001) layers. The free electron concentrations: (a) 4.2×10^{16} , (b) 3.1×10^{17} , (c) 2.1×10^{18} , (d) 4.8×10^{16} , (e) 2.1×10^{17} , and (f) 4.7×10^{17} cm^{-3} .

The addition of DETe to the system also has a dramatic effect of the surface structure, observed using the AFM. For the singular (001) orientation, a mound structure (or wedding cake morphology) is formed for the undoped GaInP layers. This is commonly attributed to the formation of a barrier to adatom attachment at “down” steps on the surface.²² The mounds are elongated in the [110] direction, indicating that the step velocity during growth is higher for $[\bar{1}10]$ than for [110] steps. The three-dimensional (3D) structure is completely eliminated for Te doping levels exceeding 10^{18} cm^{-3} ,¹⁶ resulting in a surface that is atomically flat except for widely (approximately 1 μm) spaced monolayer

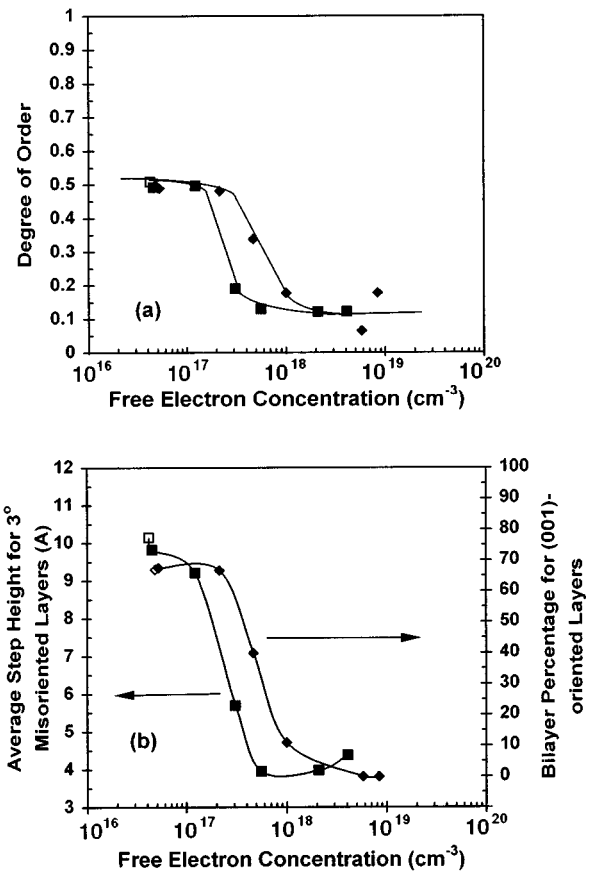


FIG. 3. (a) Degree of order vs electron concentration from Te doping. (b) Percentage of bilayer steps and average step height as a function of electron concentration. Te-doped GaInP singular (001) layers (\blacklozenge) and vicinal layers (\blacksquare) were grown at 670 °C. The lines were simply drawn to fit the data points.

steps due to the slight unintentional local misorientation of the surface. The $[\bar{1}10]$ step spacing is also increased by a factor of approximately 20 indicating a marked increase in step velocity during growth due to Te doping. In addition, the steps around the perimeter of the islands change from predominately bilayers (5.8 Å in height) to completely monolayers as the Te doping level is increased, as shown in Fig. 3(b).

For undoped GaInP layers grown by OMVPE on vicinal GaAs substrates, step bunching is well documented.²³ The undoped layers grown in this study exhibited this phenomenon with average step heights of 10 Å. The steps were monolayers at high Te doping levels, as seen in Fig. 3(c).

IV. DISCUSSION

A considerable amount of information about the effect of growth parameters on step structure has been published that is relevant to this discussion. Considering first undoped material, grown on singular (001) substrates using conditions similar to those used in this study, which results in highly ordered material, the steps are reported to be mainly bilayer, with a small amount of step bunching.²⁴ For growth on 3°_B vicinal substrates at 620 °C the average step height was reported to be 6 Å;²⁴ however, the current data, obtained at 670 °C, give a slightly larger value of 10 Å.

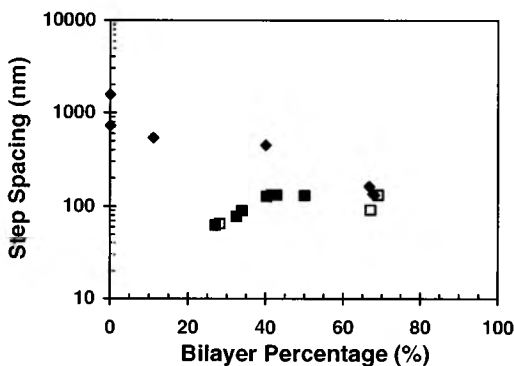


FIG. 4. $[\bar{1}10]$ step spacing vs percentage of bilayer steps for singular (001) GaInP layers grown at 670 °C. The diamond symbols (◆) were obtained by changing the Te doping level with a fixed 3.0 Torr TBP partial pressure. The square symbols were obtained by changing the group V partial pressure from 0.75 to 9.0 Torr, using either TBP (□) or PH_3 (■) in undoped GaInP.

The islands on singular (001) substrates in undoped material are elongated, indicating a higher velocity for $[\bar{1}10]$ than for $[110]$ steps.²⁵ The effect of decreasing the TBP partial pressure has been reported to be a decrease in step velocity (or step spacing) for the monolayer steps produced.²⁶ The step spacing from this study is plotted versus the percentage of bilayer steps in Fig. 4.

The effect of the addition of Te at levels of $\geq 10^{18} \text{ cm}^{-3}$ is a change from bilayer to monolayer steps for the singular (001) orientation¹⁶ and the elimination of step bunching for vicinal substrates misoriented to produce $[110]$ steps.¹⁷ For singular substrates, the $[\bar{1}10]$ step velocity is increased by a factor of 20 when Te is added to the system¹⁶ and the mound structure observed for the undoped layers disappears. These data are included in Fig. 4. A comparison of the dissimilar effects due to changing the partial pressure of the group V precursor and of the addition of Te to the system seen in Fig. 4 clearly indicates that the effect of Te doping is not simply due to a change in the step structure from bilayer to monolayer.

A remarkable coincidence between the changes in the degree of order and the step structure as the Te doping level is increased can be clearly seen by a comparison of the data in Figs. 3(a) and 3(b). The changes in both occur over exactly the same range of Te doping. The surface reconstruction is found to be unchanged by Te doping at levels much larger than those required to eliminate ordering.¹⁶ This strongly suggests that the step structure change induced by the addition of Te to the system is responsible for the change in the degree of CuPt ordering, rather than a reduction in the surface thermodynamic driving force for ordering.

The remainder of this section will be devoted to a discussion of how Te doping affects the step structure, as well as the effect(s) of the step structure on the formation of the CuPt structure at the surface during growth.

Consider first the effects of growth parameters on the step structure of undoped GaInP layers. The formation of bilayer steps at high values of the partial pressure of the P precursor (p_P) is attributed to the reduction in step energy due to the elimination of dangling bonds by formation of a

(2×2) reconstruction on the thin ribbon of $\{111\}$ material formed at the bilayer step edge.²⁴ The structures, with P trimers sitting on top of P atoms for $[110]$ bilayer steps and on top of group III atoms for $[\bar{1}10]$ bilayer steps, are illustrated in Figs. 5(a) and 5(b). Both structures obey the electron counting rule,²⁷ so are expected to have no dangling bonds. Examination of the diagram in Fig. 5(a) indicates that for $[110]$ steps a group III adatom (termed simply adatom in what follows) approaching the step edge will find the group III site either already occupied by a P atom belonging to the P trimer or surrounded by P atoms without electrons to make bonds to the adatom. Clearly, the ability of an adatom approaching the step edge to be strongly attached will be small for this atomic configuration. An examination of Fig. 5(a) indicates that the same problem is encountered for group III adatoms approaching the step from either the upper or the lower (001) terrace. The qualitative similarity of the attachment processes at “up” and “down” steps suggests approximately equal sticking coefficients. As discussed later, the presence of a large Ehrlich–Schwoebel barrier, resulting in a low sticking coefficient at down steps, leads to step ordering rather than bunching. If the sticking coefficients are approximately equal, the bilayer steps will not bunch,^{28,29} in agreement with the experimental observations.

For adatoms approaching a $[\bar{1}10]$ step edge, the sticking coefficients for both the upper and lower terraces would appear to be higher than for the $[110]$ steps, explaining the elongation of the islands in the $[110]$ direction. As indicated in Fig. 5(b), the group III adatom arriving at the step edge where the P trimer is present will find the site vacant and surrounded by 3 P neighbors. Thus, a P atom will not have to be displaced before the adatom can be attached at the step. However, a high sticking coefficient is not expected. The electrons in the P atoms on the surface trimer are all accounted for by formation of back bonds, trimer bonds, and lone pairs, as indicated in Fig. 5(b), since the (2×2) reconstruction satisfies the electron counting rule. Again, this simple model is consistent with sticking coefficients at up and down steps that are comparable in magnitude.

For lower values of p_P in undoped GaInP, monolayer steps form and it seems likely that the “dangling” P site at the $[\bar{1}10]$ step edge will be vacant due to the low P surface coverage. This probably accounts for the adatom sticking coefficient being even lower than for the bilayer steps formed at higher values of p_P in the undoped material, illustrated by the data in Fig. 4.

The relatively low sticking coefficients at the monolayer and bilayer step edges in undoped material increase the opportunity for formation of the ordered structure, provided that a surface thermodynamic driving force exists due to a high concentration of $[\bar{1}10]$ oriented P dimers on the (001) surface.

The effect of Te on the step structure is believed to be mainly caused by the destabilization of the (2×2) reconstruction at the $\{111\}$ A and $\{111\}$ B step edges. The Te added to the system is postulated, due to observed behavior during molecular-beam epitaxy growth,³⁰ to collect at the surface and, particularly, at the step edge. The extra valence

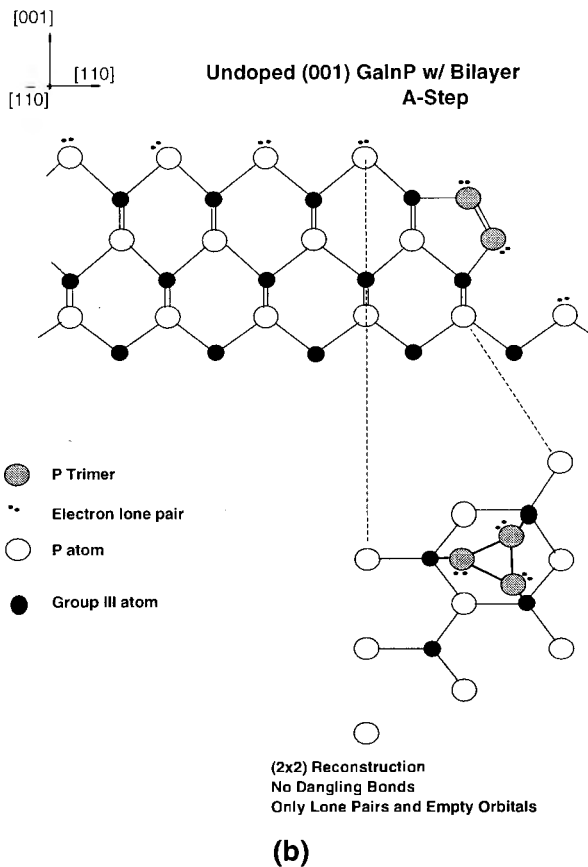
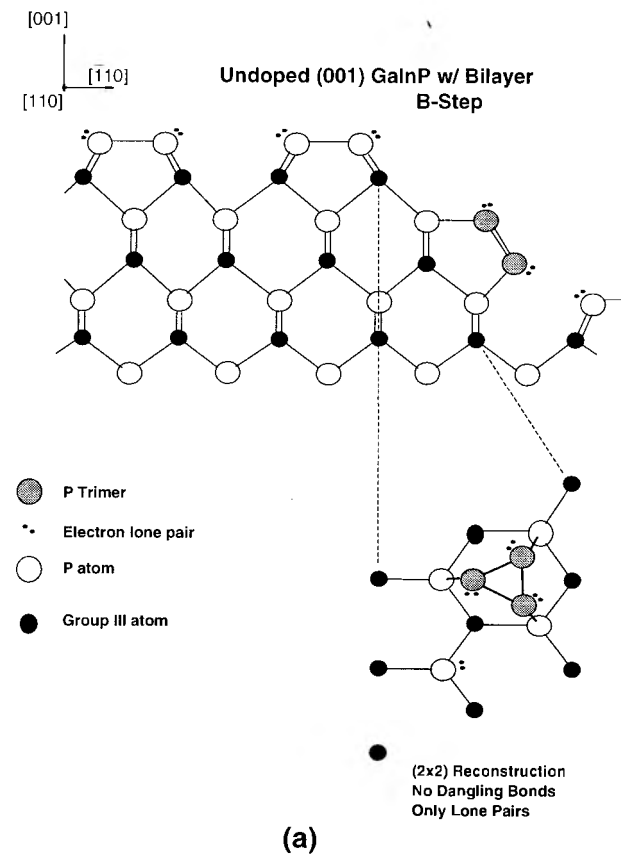


FIG. 5. Schematic cross-sections of (a) [110] and (b) $[\bar{1}10]$ steps, without Te doping. Bilayer steps with the P-trimer (2×2) reconstructions at the step edges are shown.

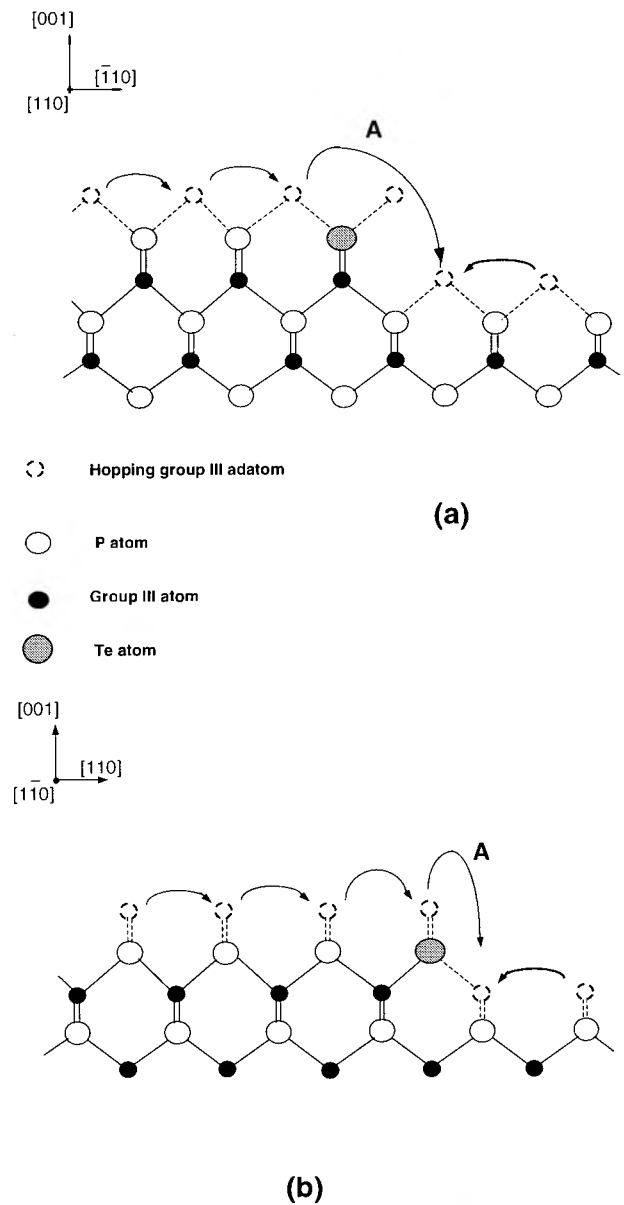


FIG. 6. Schematic cross-sections of (a) [110] and (b) $[\bar{1}10]$ steps with high Te doping levels. Monolayer steps are postulated to have a relatively low sticking coefficient for attachment at down steps, as indicated by the pathway labelled "A."

electron of Te, relative to the P which it replaces, will certainly change the electron counting at the surface and thus, presumably, at high concentrations, remove the driving force for formation of the (2×2) structure shown in Figs. 5(a) and 5(b) at the step edges. Obviously, the electron counting rule will no longer be satisfied for these reconstructions. It is this factor that is postulated to result in the formation of monolayer steps on singular surfaces, as observed experimentally. Presumably, the dangling bonds due to Te on the $(11\bar{n})$ surface formed at the edge of a bunched step might also destabilize the structure formed by step bunching for growth on vicinal surfaces. This would be in addition to kinetic effects at monolayer step edges, discussed later, that would reduce or eliminate step bunching.

An examination of the schematic monolayer step structures shown in Fig. 6(b) indicates that the adatom sticking

coefficient at the $[\bar{1}10]$ step edge from the lower terrace will probably be large due to the formation of 3 bonds. This assumes that the dangling P site is occupied, which is reasonable for the values of p_P and growth temperature used, and ignores reconstruction of the atoms at the step edge. [Note that the sticking coefficient is expected to be low at monolayer step edges in undoped materials, as discussed earlier. However, this is due to the very low values of p_P required to destabilize the (2×2) reconstruction at the step edge in undoped material, which will result in the dangling P site being unoccupied.] The experimental data clearly show that, indeed, the sticking coefficient is high at the $[\bar{1}10]$ monolayer step edge for the conditions used for the growth of the Te doped layers in this study: The step velocity is more than an order of magnitude higher than for bilayer steps in undoped material,¹⁶ as seen in Fig. 4. The increase in sticking coefficient acts directly to decrease the degree of CuPt order. For example, a unity sticking coefficient would yield a totally disordered alloy. The large amount of Ga–In exchange necessary to form the lower energy ordered structure at the surface in the short time before the surface is covered by the following layer suggests that a very low sticking coefficient is required to form layers with the high degree of order (approximately 0.5) observed experimentally.

Examination of the model of $[\bar{1}10]$ monolayer steps in Fig. 6(b) indicates that the sticking coefficient will be high *only* for up steps. For attachment at $[\bar{1}10]$ steps from the upper terrace (at down steps), the adatom will apparently have to transit an intermediate position where the adatoms are attached solely to the P (or Te) at the dangling sites. This is expected to result in a significant Ehrlich–Schwoebel barrier and, as a consequence, a lower value of sticking coefficient at the down steps than that at up steps. Similarly, the illustration of the $[110]$ monolayer step in Fig. 6(a) indicates again that a step edge potential barrier will exist for attachment at down steps since the adatoms must occupy a transition state bonded to a single P (or Te) atom.³¹ This kinetic effect would add to the thermodynamic effect described above accounting for the total elimination of step bunching observed.

One additional piece of data relating to the effect of step structure on the velocity and degree of CuPt ordering is also of interest here. Lee *et al.*²⁶ found that the change from TBP to PH_3 as the P precursor resulted in a significant increase in the number of monolayer steps. However, this change from bilayer to monolayer steps had no effect on the step spacing (step velocity). This was attributed to the effect of H adsorbed at the step edge to passivate the dangling bonds for growth using PH_3 where the H coverage of the surface is expected to be larger than for growth using TBP. Thus, the results are consistent with the data and interpretations presented here. Since the step velocity was not increased, the change from bilayer to monolayer steps had no observable effect on the degree of CuPt order.

Finally, the elimination of 3D islands (or mounds) for the growth of Te doped GaInP on “singular” (001) substrates is directly attributed to the high adatom sticking co-

efficient at $[\bar{1}10]$ monolayer steps (and kink sites on $[110]$ monolayer steps) from the lower terrace. The resultant increase in the step spacing at the island edges now exceeds the “natural” step spacing due to the slight, unintentional misorientation from (001). Assuming that the adatom diffusion length exceeds the natural step spacing,³² this leads to step-flow growth.

V. CONCLUSIONS

The addition of Te to the GaInP system during OMVPE growth causes several significant changes. It causes an increase in band gap energy. This is attributed to a reduction in the CuPt order parameter observed from electron diffraction results. Over the same range of Te doping that destroys CuPt order the surface structure also changes markedly: the bilayer steps observed for undoped layers for growth on singular (001) substrates “dissociate” into monolayer steps. At the same time, the $[\bar{1}10]$ step velocity increases by a factor of $20\times$ and the 3D mound structure disappears. For growth on vicinal substrates, intentionally misoriented to produce $[110]$ steps on the surface, the step bunching observed in undoped layers disappears as the Te doping level is increased. AFM images show that surfaces for growth on both substrate orientations become extremely smooth as the Te doping level is increased. The coordinated change in CuPt order parameter and step structure with increased Te doping suggests that the change in step structure causes the change in ordering. Earlier reports showed no change in surface reconstruction over this range of Te doping level.

A model is presented that rationalizes the change in step structure caused by Te doping. The high adatom sticking coefficient at the monolayer $[\bar{1}10]$ steps formed due to Te doping leads directly to the loss of CuPt ordering. This also results in the elimination of 3D mounds on the surface during growth by the addition of Te, since steps are present due to unintentional substrate misorientation. The change in the relative sticking coefficients at up and down steps due to the transition from bilayer steps terminated by (2×2) reconstructed surfaces to monolayer steps may be responsible for the reduction in step bunching. Thermodynamic destabilization of the $(11n)$ facet at the bunched step edge may also play a role.

ACKNOWLEDGMENTS

This work was sponsored by the National Science Foundation (growth and AFM step structure studies) and the Department of Energy (PL and electron microscopy studies).

¹G. B. Stringfellow, in *Thin Films: Heteroepitaxial Systems*, edited by M. Santos and W. K. Liu (World Scientific Publishing) (to be published).

²G. B. Stringfellow, in *Common Themes and Mechanisms of Epitaxial Growth*, edited by P. Fuoss, J. Tsao, D. W. Kisker, A. Zangwill, and T. Kuech (Materials Research Society, Pittsburgh, 1993), pp. 35–46.

³N. Kobayashi, Y. Kobayashi, and K. Uwai, *J. Cryst. Growth* **174**, 544 (1997).

⁴S. B. Zhang, S. Froyen, and A. Zunger, *Appl. Phys. Lett.* **67**, 3141 (1995).

⁵H. Murata, I. H. Ho, L. C. Su, Y. Hosokawa, and G. B. Stringfellow, *J. Appl. Phys.* **79**, 6895 (1996).

⁶L. C. Su, I. H. Ho, N. Kobayashi, G. B. Stringfellow, *J. Cryst. Growth* **145**, 140 (1994).

- ⁷R. P. Schneider, E. D. Jones, and D. M. Follstaedt, *Appl. Phys. Lett.* **65**, 587 (1994).
- ⁸H. Murata, I. H. Ho, Y. Hosokawa, and G. B. Stringfellow, *Appl. Phys. Lett.* **68**, 2237 (1996).
- ⁹A. Gomyo, Hitoshi Hotta, Isao Hino, S. Kawata, Kenichi Kobayashi, and Tohru Suzuki, *Jpn. J. Appl. Phys., Part 2* **28**, L1330 (1989).
- ¹⁰J. P. Goral, Sarah R. Kurtz, J. M. Olson, and A. Kibbler, *J. Electron. Mater.* **19**, 95 (1990).
- ¹¹T. Suzuki, A. Gomyo, I. Hino, K. Kobayashi, S. Kawata, and S. Iijima, *Jpn. J. Appl. Phys., Part 2* **27**, L1549 (1988).
- ¹²F. P. Dabkowski, P. Gavrilovic, K. Meehan, W. Stutius, J. E. Williams, M. A. Shahid, and S. Mahajan, *Appl. Phys. Lett.* **52**, 2142 (1988).
- ¹³E. Morita, M. Ikeda, O. Kumagai, and K. Kaneko, *Appl. Phys. Lett.* **53**, 2164 (1988).
- ¹⁴M. K. Lee, R. H. Horng, and L. C. Haung, *Appl. Phys. Lett.* **59**, 3261 (1991).
- ¹⁵Sarah R. Kurtz, J. M. Olson, D. J. Friedman, A. E. Kibbler, and S. Asher, *J. Electron. Mater.* **23**, 431 (1994).
- ¹⁶S. H. Lee, T. C. Hsu, and G. B. Stringfellow, *J. Appl. Phys.* **84**, 2618 (1998).
- ¹⁷S. H. Lee, C. F. Fetzer, and G. B. Stringfellow, *J. Cryst. Growth* **195**, 13 (1998).
- ¹⁸P. Ernst, C. Geng, F. Scholz, H. Schweizer, Y. Zhang, and A. Mascarenhas, *Appl. Phys. Lett.* **67**, 2347 (1994).
- ¹⁹J. I. Pankove, *Optical Processes in Semiconductors* (Dover Publications, Inc., New York, 1971), pp. 134–137.
- ²⁰P. Ernst, Y. Zhang, F. A. J. M. Driessen, A. Mascarenhas, E. D. Jones, C. Geng, F. Scholz, and H. Schweizer, *J. Appl. Phys.* **81**, 2814 (1997).
- ²¹L. C. Su, I. H. Ho, and G. B. Stringfellow, *J. Appl. Phys.* **75**, 5135 (1994).
- ²²A. Zangwill, *J. Cryst. Growth* **163**, 8 (1996).
- ²³G. B. Stringfellow and L. C. Su, *J. Cryst. Growth* **163**, 128 (1996).
- ²⁴Y. S. Chun, H. Murata, T. C. Hsu, I. H. Ho, L. C. Su, Y. Hosokawa, and G. B. Stringfellow, *J. Appl. Phys.* **79**, 6900 (1996).
- ²⁵S. H. Lee and G. B. Stringfellow, *J. Appl. Phys.* **83**, 3620 (1998).
- ²⁶S. H. Lee, Yu Hsu, and G. B. Stringfellow, *J. Electron. Mater.* **26**, 1244 (1997).
- ²⁷M. D. Pashley, *Phys. Rev. B* **40**, 10481 (1989).
- ²⁸S. A. Chalmers, J. Y. Tsao, and A. C. Gossard, *Appl. Phys. Lett.* **61**, 645 (1992).
- ²⁹C. Orme, M. D. Johnson, K. T. Leung, B. G. Orr, P. Smilauer, and D. Vvedensky, *J. Cryst. Growth* **150**, 128 (1995).
- ³⁰A. Ferraz and R. C. de Silva, *Surf. Sci.* **352–354**, 379 (1996).
- ³¹Y. Tokura, H. Saito, and T. Fukui, *J. Cryst. Growth* **94**, 46 (1989); G. Ehrlich and F. G. Hudda, *J. Chem. Phys.* **44**, 1039 (1966); R. L. Schwoebel, *J. Appl. Phys.* **40**, 614 (1969).
- ³²M. Hata, T. Isu, A. Watanabe, Y. Kajikawa, and Y. Katayama, *J. Cryst. Growth* **114**, 203 (1991); T. Isu, M. Hata, Y. Morishita, Y. Nomura, and Y. Katayama, *ibid.* **115**, 423 (1991).